Durham University

Durham Research Online

Deposited in DRO:

24 May 2011

Version of attached file:

Published Version

Peer-review status of attached file:

Peer-reviewed

Citation for published item:

Wacher, Abigail and Seymour, Brian (2011) 'A radiation model of a rapid thermal processing system.', Mathematics-in-industry case studies., 3 . pp. 1-18.

Further information on publisher's website:

http://www.fields.utoronto.ca/journalarchive/mics/35.html

Publisher's copyright statement:

Additional information:

Use policy

The full-text may be used and/or reproduced, and given to third parties in any format or medium, without prior permission or charge, for personal research or study, educational, or not-for-profit purposes provided that:

- a full bibliographic reference is made to the original source
- a link is made to the metadata record in DRO
- the full-text is not changed in any way

The full-text must not be sold in any format or medium without the formal permission of the copyright holders.

Please consult the full DRO policy for further details.

Durham University Library, Stockton Road, Durham DH1 3LY, United Kingdom
Tel : +44 (0)191 334 3042 | Fax : +44 (0)191 334 2971
https://dro.dur.ac.uk

MICS JOURNAL

Mathematics-in-Industry Case Studies Journal, Volume 3, pp. 1-18 (2011)

A Radiation Model of a Rapid Thermal Processing System

Abigail Wacher * Brian R. Seymour †

Abstract. A model of the radiative heat transfer that takes place in an axially symmetric rapid thermal processing chamber is presented. The model is derived using the theory of shape factors, and is used to predict how chamber geometry and materials affect temperature uniformity on the processed silicon wafer. Using a series of numerical experiments we predict the effects on the temperature uniformity of the size and reflectivity of the showerhead, the guard ring, and the chamber height.

Keywords. Radiation, Modelling, Rapid Thermal Processing, Industrial mathematical modelling.

1 Introduction

A Rapid Thermal Processing (RTP) system processes silicon wafers to make semiconductors for computer devices and high speed computation applications. Annealing is a process used to add impurities to the semiconductor by the method of thermally-activated diffusion. Rapid thermal processing (RTP) is one technology for thermally-activated diffusion. Temperature uniformity of the wafer during the annealing process is important to obtain uniform conductivity and resistivity throughout the wafer. The RTP method has two advantages over conventional furnace annealing: it lowers the thermal budget (integral of time and temperature) and produces superior oxides and silicides.

The RTP system studied here was designed by the Vancouver based company Vortek Industries Limited, founded in 1976 as a spin-off company from the University of British Columbia. Modeling the Vortek RTP formed the basis of the first author's MSc in industrial mathematics, at the University of British Columbia, under the organization of PIMS/MITACS.

Inside the RTP chamber is a silicon wafer that is heated to hundreds of degrees Celsius in a few seconds, primarily through radiation. A model is derived that predicts how chamber geometry

*Durham University, Department of Mathematical Sciences, Durham, DH1 3LE, United Kingdom, abigail.wacher@durham.ac.uk

†Department of Mathematics, University of British Columbia, Vancouver, V6T 1Z2, Canada, seymour@math.ubc.ca

and materials affect temperature uniformity on the wafer during a process run with no gas flowing inside the chamber. Vortek data between 1999 and 2000 is used in the model.

Knowing the irradiation from below the wafer and that the temperature at the showerhead above the wafer is held constant, we calculate the temperature on the wafer using a heat balance equation at the wafer. In this calculation we take into account the radiative heat exchange between the wafer and the showerhead, which is derived from shape factor (or view factor) theory. The radiative heat exchange is modeled using shape factors resulting in a system of linear equations with irradiations as the unknowns. The linear system is solved using a classic LU matrix decomposition with partial pivoting called Crout's method. The information from the solution of the linear system is then inserted into a heat balance equation. The heat balance equation is then solved analytically to obtain an explicit function of temperature and time step. This equation is then solved numerically using Newton's method to obtain a temperature after one time step.

2 Physical model

A simple schematic of the Vortek chamber is shown in Figure 1. Light shines from a (200 kW) arc lamp through a quartz window positioned in such a way that the light shines uniformly on the bottom surface of the silicon wafer. The chamber shown contains a thin silicon wafer placed so that it divides the chamber into two compartments. The upper compartment has a highly reflective metal grid (showerhead) above the wafer. Gas may be injected into the chamber using the showerhead. The wafer has a guard ring (there is a small space between the wafer and the guard ring) that helps maximize the temperature uniformity on the wafer surface by blocking energy reflections from the chamber walls. The lower compartment is a black cavity, that absorbs all reflected radiation from the wafer, thus preventing it from reflecting back to the wafer. The arc lamp (Vortek's water-wall arc-lamp), is mounted in a reflector so that the radiation reflected and emitted from the wafer is minimized and totally absorbed by the cavity walls. Most of the radiative energy that is emitted from the upper surface of the wafer strikes the surface of the showerhead. Some of this energy is absorbed (30%) and the rest is reflected back to the wafer surface.

The wafer is typically 200mm in diameter and 0.7mm thick. The wafer is heated from below from room temperature to a maximum temperature of 1050 °C. A cooling gas (nitrogen) can be injected into the upper compartment from the showerhead which is made of hand polished aluminum with a reflectivity of about 0.7. The showerhead is water cooled, and kept at a constant temperature of about room temperature to approximately 100 °C. Note that the emissivity of the showerhead is important and must be included. The gap between the showerhead and the surface of the wafer is adjustable from 2 mm to 5cm; at present it is set at 1 cm. The cooling gas is injected with a flow rate that may vary from zero upward, but a good value is 10 standard liters per minute (no preheating, but this is variable). The gas flows down and through the upper compartment and out of the chamber, upward through the outlet placed between the showerhead and the chamber walls.

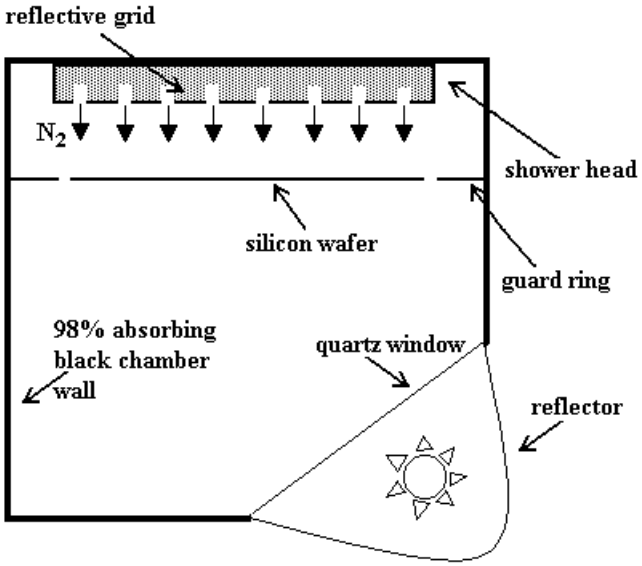

Figure 1: *Vortek chamber*

Physical assumptions

Some physical assumptions and geometry simplifications must be made to make this study possible given the time and tools available. Once these assumptions have been made one can define a computational domain. The following is a description of the simplified computational domain.

The light intensity from the lamp is assumed to be uniform at the wafer lower surface. The silicon wafer will be assumed infinitely thin in the sense that the temperature on the top surface of the wafer will be assumed identical to the temperature on the lower surface. The chamber has an axially symmetric geometry. A linear approximation is used for the temperature gradient at the bottom and top surfaces of the wafer. The cooled walls and the showerhead are assigned a fixed temperature boundary condition. The total hemispherical emissivity is approximated to 0.68, which is the emissivity at temperatures above approximately 700 °C obtained from [5].

3 Development of the radiation model

"Thermal radiation is the term used to describe the electromagnetic radiation which has been observed to be emitted at the surface of a body which has been thermally excited. This electromagnetic radiation is emitted in all directions; and when it strikes another body, part may be reflected, part may be transmitted, and part may be absorbed.", cf. [2]. For a given surface we define:

W = emissive power, i.e., total emitted thermal radiation leaving a surface, per unit area. $W = \epsilon\sigma T^4$, where T is the given temperature of the surface, σ is the Stefan-Boltzmann constant and ϵ is the total hemispherical emissivity at that temperature. For a given temperature the emissivity ϵ may have a value between 0 and 1 and is characteristic of the material. Black surfaces have emissivity close to unity and thus emit more radiation than shiny surfaces that have emissivity close to zero.

J = radiosity, i.e., total thermal radiation leaving the surface, per unit surface area. Radiosity includes the original emitted radiation plus the reflected radiation.

G = irradiation, i.e., total thermal radiation incident upon the surface per unit surface area and is the result of the emitted radiation and reflections from other surfaces.

The relation between the energy that is absorbed, reflected and transmitted by a material is given by the law of conservation of energy:

$$\alpha + r + \tau = 1, \tag{1}$$

where

α = absorptivity, i.e., the fraction of the incident radiation absorbed.

r = reflectivity. i.e., the fraction of the incident radiation reflected.

τ = transmissivity, i.e., the fraction of the incident radiation transmitted through the body.

Absorptivity, reflectivity and transmissivity are temperature dependant variables that also depend on the surface characteristics, structure, material, and the wavelength of the incident radiation. For each surface considered here α, r and τ will be taken as constants given that the surfaces are flat and opaque, and the incident radiation has a dominant wavelength. Since the surfaces are opaque, $\tau = 0$, and so at each surface: $\alpha + r = 1$. In addition to this information we will need a corollary of Kirchhoff's law that states that at thermal equilibrium the absorptivity and the emissivity of any body are equal, or $\alpha = \epsilon$. This means that surfaces that emit less radiation also absorb less of the radiation incident upon the surface, and so most of the incident radiation is reflected. However, darker surfaces with large emissivity absorb more of the incident radiation and thus are less reflective.

We label a surface A_i as the surface which has an area A_i, where the surface considered is either a disk or a ring. Without loss of generality we will use the label A_i to refer to the surface as well as the actual area of the surface. The shape, or configuration factor, from A_1 to A_2, written F_{12}, may be defined as the fraction of the total radiant energy leaving A_1 that is incident upon A_2. The shape factor is a function of the geometry of the two surfaces A_1 and A_2 and also depends on the directional distribution of the radiation from the source. For the purpose of this paper the directional distribution of the radiant emission has been assumed to follow Lambert's cosine law. The shape factor material used in this paper has been extracted from [2] and [3].

The shape factor for a disk A_1 of radius r_1 which is parallel to a disk A_2 of radius r_2 is:

$$F_{12} = \frac{1}{2}(x - \sqrt{x^2 - 4E^2D^2}), \tag{2}$$

where $E = r_2/d, D = d/r_1$, $x = 1 + (1 + E^2)D^2$, and d is the distance between surface A_1 and A_2.

Now consider two parallel disks, A_{12} with radius r_2 and A_{34} with radius r_3, be subdivided as follows. Let A_1 be a disk with radius r_1 and A_2 be a ring which has an inner radius r_1 and an outer radius r_2 (containing A_1). The disk formed by the union of the surfaces A_1 and A_2 is A_{12}. Similarly disk A_{34} is the union of two surfaces A_3 and A_4, where A_4 is a disk of radius r_4 and A_3 is a ring with inner radius r_4 and an outer radius r_3 (containing A_4). We can then calculate the shape factor from the disk A_1 to A_4 as F_{14} and similarly we can calculate the shape factor from the disk A_{12} to the disk A_4 as $F_{(12)4}$. Using the basic reciprocity and decomposition laws for shape factors, we derive the shape factor from a ring A_2 to a disk A_4:

$$F_{24} = \frac{A_1 + A_2}{A_2}F_{(12)4} - \frac{A_1}{A_2}F_{14}. \tag{3}$$

Similarly we obtain the relation from a ring A_2 to a ring A_3, F_{23}:

$$F_{23} = \frac{1}{A_2}\{(A_1 + A_2)[F_{(12)(34)} - F_{(12)4}] - A_1[F_{1(34)} - F_{14}]\ \}. \tag{4}$$

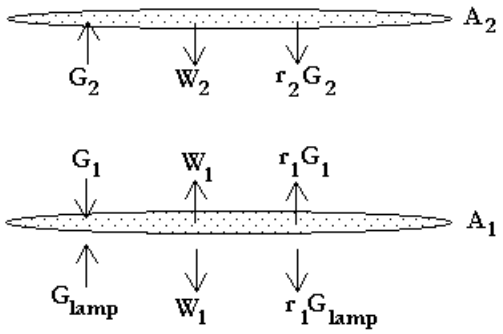

Figure 2: *Radiation exchange between two parallel surfaces including lamp*

3.1 Radiation exchange equations

Assuming the space between the two parallel surfaces shown in Figure 2 is filled with nitrogen, and assuming that the thermal radiation passes through it as though in a vacuum, then the transmissivity is unity, i.e., $\alpha = r = 0$. Further assume that surface A_2 is cooled so that it is maintained at a constant temperature, then the equation for the total radiant energy leaving a surface is:

$$J = W + rG = W + (1 - \alpha)G. \tag{5}$$

So for A_1 and A_2 where the gas is nitrogen, the heat exchange due to radiation can be described as:

$$J_1 = W_1 + (1-\epsilon_1)G_1 = \epsilon_1\sigma T_1^4 + (1-\epsilon_1)G_1. \tag{6}$$

$$J_2 = W_2 + (1-\epsilon_2)G_2 = \epsilon_2\sigma T_2^4 + (1-\epsilon_2)G_2. \tag{7}$$

The energy leaving surface A_2 that eventually strikes surface A_1 is given by $A_2F_{21}J_2$, where F_{12} is the shape factor based on the area of disk A_1. G_1 is the radiant energy leaving surface A_2 that strikes A_1 per unit surface area, and is thus equal to $A_2F_{21}J_2/A_1 = F_{12}J_2$. Applying the same principles at A_2: G_2 is the radiant energy leaving surface A_1 that strikes A_2 per unit surface area, and is thus equal to $F_{21}J_1$,where F_{21} is the shape factor based on the area of disk A_2.

Inserting G_1 and G_2 into the radiant energy equations results in two equations for two unknowns: J_1 and J_2:

$$\begin{aligned} J_1 &= \epsilon_1\sigma T_1^4 + (1-\epsilon_1)F_{12}J_2, \\ J_2 &= \epsilon_2\sigma T_2^4 + (1-\epsilon_2)F_{21}J_1. \end{aligned} \tag{8}$$

If we further subdivide each of A_1 and A_2 into a finite number of rings (not necessarily of equal width and each surface may be subdivided into a different number of rings), we then get the following formulae for the corresponding radiative system:

$$\begin{aligned} J_{1_i} &= \epsilon_{1_i}\sigma T_{1_i}^4 + (1-\epsilon_{1_i})G_{1_i} \quad \text{for } i = 1, ..., n, \\ J_{2_j} &= \epsilon_{2_j}\sigma T_{2_j}^4 + (1-\epsilon_{2_j})G_{2_j} \quad \text{for } j = 1, ..., m. \end{aligned} \tag{9}$$

$\epsilon_{2j} = \epsilon_{\text{showerhead}}$ will be constant for all j. {Note, When the ring in consideration is an inflow, $\tau \neq 0$ as assumed above but rather $\tau = 1$, in which case $\alpha = 0, r = 0$, and thus at an inflow $J_{1_i} = 0$.}

$\epsilon_{1_i} = \epsilon_{\text{silicon}}$ will be constant for all i.

T_{2_j} will be constant for each j.

$T_{1_i} = T_{1_i}(t)$.

If we replace G_{1_i} and G_{2_j} using the reciprocity and decomposition laws for shape factors:

$$\begin{aligned} J_{1_i} &= \epsilon_{1_i}\sigma T_{1_i}^4 + (1-\epsilon_{1_i})\textstyle\sum_{j=1}^{m} F_{1_i2_j}J_{2_j} \quad \text{for } i = 1, ..., n, \\ J_{2_j} &= \epsilon_{2_j}\sigma T_{2_j}^4 + (1-\epsilon_{2_j})\textstyle\sum_{i=1}^{n} F_{2_j1_i}J_{1_i} \quad \text{for } j = 1, ..., m. \end{aligned} \tag{10}$$

Note that $F_{2_j1_i}, F_{1_i2_j}$ will be constant for each i and each j. The above is a system consisting of $(n+m)$ linear coupled equations and $(n+m)$ unknowns: $J_{1_1}, J_{1_2}, J_{1_3}, ..., J_{1_n}, J_{2_1}, ..., J_{2_m}$.

3.2 Heat balance equation at the wafer

Given that we know the irradiation from below a surface A_1 (from the lamp) as in Figure 2, and that the temperature at surface A_2 is held constant, and assuming that A_1 (the silicon wafer) is infinitely thin, we may calculate at each step in time the temperature at surface A_1. This is achieved by looking at the radiative heat exchange between the two surfaces, solving for the irradiation on each A_{1_i} (by solving the radiative system of equations) and advancing the temperature at each A_{1_i} in time by using the following heat balance equation at A_{1_i}:

$$\begin{aligned}\rho_{\mathsf{Si}} C_{p_{\mathsf{Si}}} h_{\mathsf{Si}} \frac{\partial T_{1_i}}{\partial t} &= G_{1_1} + G_{\text{lamp}} - 2W_{1_i} - r_{1_i} G_{1_i} - r_{1_i} G_{\text{lamp}} \\ &\quad + k_{\mathsf{N}} \frac{\partial T_{1_i}}{\partial y}\bigg|_{aw} - k_{\mathsf{N}} \frac{\partial T_{1_i}}{\partial y}\bigg|_{bw} \quad \text{for } i = 1, ..., n,\end{aligned} \tag{11}$$

where h_{Si} is the thickness of the wafer, ρ_{Si} is the density of silicon, $C_{p_{\mathsf{Si}}}$ is the heat capacity of silicon, and k_{N} is the conductivity of nitrogen.

The first term on the left hand side of the equation represents the change of energy of A_{1_i} with respect to time. On the right hand side of the equation are the seven terms representing the incoming and outgoing energy at A_{1_i}. The positive terms represent the incoming energy and the negative terms represent the outgoing energy. The first term G_{1_1} is the total thermal radiation incident on A_{1_i} from above, per unit surface area. G_{lamp} is the total thermal radiation incident on A_{1_i} from the lamp below, per unit surface area. W_{1_i} is the total emitted thermal radiation leaving each side (surface) of A_{1_i} per unit area, and so this term is included twice. $r_{1_i} G_{1_i}$ is the total thermal radiation reflected at the top surface of A_{1_i}, per unit surface area. $r_{1_i} G_{\text{lamp}}$ is the total thermal radiation reflected at the bottom surface of A_{1_i}, per unit surface area. $\partial T_{1_i}/\partial y_{aw}$ is the temperature gradient above the wafer at A_{1_i} and $\partial T_{1_i}/\partial y_{bw}$ is the temperature gradient below the wafer at A_{1_i}. The values used for h_{Si}, ρ_{Si}, $C_{p_{\mathsf{Si}}}$, k_{N}, $\partial T_{1_i}/\partial y_{aw}$ and $\partial T_{1_i}/\partial y_{bw}$ are discussed in the following section. Replacing r_{1_i} with $(1 - \epsilon_{1_i}), W_{1_i}$ with $\epsilon_{1_i} \sigma T_{1_i}^4$ and G_{1_i} with $\sum_{j=1}^{m} F_{1_i 2_j} J_{2_j}$ we obtain the following simplified equation:

$$\begin{aligned}\rho_{\mathsf{Si}} C_{p_{\mathsf{Si}}} h_{\mathsf{Si}} \frac{\partial T_{1_i}}{\partial t} &= \epsilon_{1_i} \sum_{j=1}^{m} F_{1_i 2_j} J_{2_j} + \epsilon_{1_i} G_{\text{lamp}} - 2\epsilon_{1_i} \sigma T_{1_i}^4 \\ &\quad + k_{\mathsf{N}} \frac{\partial T_{1_i}}{\partial y}\bigg|_{aw} - k_{\mathsf{N}} \frac{\partial T_{1_i}}{\partial y}\bigg|_{bw} \quad \text{for } i = 1, ..., n.\end{aligned} \tag{12}$$

We may rewrite these as:

$$\frac{\partial T_{1_i}}{\partial t} = \frac{-2\epsilon_{1_i}\sigma}{\rho_{\mathsf{Si}} C_{p_{\mathsf{Si}}} h_{\mathsf{Si}}} \left[T_{1_i}^4 - \frac{1}{2\epsilon_{1_i}\sigma} \left(\epsilon_{1_i} \sum_{j=1}^{m} F_{1_i 2_j} J_{2_j} + \epsilon_{1_i} G_{\text{lamp}} + k_{\mathsf{N}} \frac{\partial T_{1_i}}{\partial y}\bigg|_{aw} - k_{\mathsf{N}} \frac{\partial T_{1_i}}{\partial y}\bigg|_{bw} \right) \right]. \tag{13}$$

Using the information from the previous time step, for each i and j we obtain each of: ϵ_{1_i}, ρ_{Si}, $C_{p_{\mathsf{Si}}}$, $F_{1_i 2_j}$, J_{2_j}, G_{lamp}, k_{N}, $\partial T_{1_i}/\partial y_{aw}$, and $\partial T_{1_i}/\partial y_{bw}$.

In order to be able to advance the temperature by one time step at each i, these values will be used and assumed constant in the heat balance equation at each time step. For each i, the only

variable in this equation is the temperature T_i. Since:

$$\frac{2\epsilon_{1_i}\sigma}{\rho_{\mathsf{Si}}C_{p_{\mathsf{Si}}}h_{\mathsf{Si}}} \geq 0, \tag{14}$$

let

$$B_i^4 = \frac{2\epsilon_{1_i}\sigma}{\rho_{\mathsf{Si}}C_{p_{\mathsf{Si}}}h_{\mathsf{Si}}}.$$

Since:

$$\frac{1}{2\epsilon_{1_i}\sigma}\left(\epsilon_{1_i}\sum_{j=1}^{m}F_{1_i2_j}J_{2_j} + \epsilon_{1_i}G_{\text{lamp}} + k_{\mathsf{N}}\frac{\partial T_{1_i}}{\partial y}\bigg|_{aw} - k_{Ni}\frac{\partial T_{1_i}}{\partial y}\bigg|_{bw}\right) \geq 0, \tag{15}$$

let

$$C_i^4 = \frac{1}{2\epsilon_{1_i}\sigma}\left(\epsilon_{1_i}\sum_{j=1}^{m}F_{1_i2_j}J_{2_j} + \epsilon_{1_i}G_{\text{lamp}} + k_{\mathsf{N}}\frac{\partial T_{1_i}}{\partial y}\bigg|_{aw} - k_{\mathsf{N}}\frac{\partial T_{1_i}}{\partial y}\bigg|_{bw}\right)$$

Rewriting the heat balance equation with these substitutions we arrive at the following ODE:

$$\frac{dT_{1_i}}{dt} = -B_i^4\left(T_{1_i}^4 - C_i^4\right). \tag{16}$$

We may rewrite this equation to obtain the following form that allows integration:

$$\frac{dT_{1_i}}{T_{1_i}^2 - C_i^2} - \frac{dT_{1_i}}{T_{1_i}^2 + C_i^2} = -2C_i^2B_i^4dt. \tag{17}$$

Integration over the interval $[t, t+\Delta t]$ of this equation leads to the following explicit solution of the above ODE:

$$\begin{aligned} -2C_i^2B_i^4\Delta t &= \frac{1}{2C_i}\ln\left|\frac{T_{1_i}-C_i}{T_{1_i}+C_i}\right|_{t+\Delta t} - \frac{1}{C_i}\arctan\left(\frac{T_{1_i}}{C_i}\right)_{t+\Delta t} \\ &- \frac{1}{2C_i}\ln\left|\frac{T_{1_i}-C_i}{T_{1_i}+C_i}\right|_{t} + \frac{1}{C_i}\arctan\left(\frac{T_{1_i}}{C_i}\right)_{t}. \end{aligned} \tag{18}$$

We may now advance the temperature at each A_{1_i} by one time step, using Newton's method as described in the following section.

3.3 Applying Newton's method

Since we are advancing the solution by one time step Δt the independent variable is Δt, where as t is constant, so that anything evaluated at t is a constant and we are interested in solving the equation for T_{1_i} at $t+\Delta t$. We computed solutions using a second order Runge Kutta method that is inefficient as compared to Newton's method for this particular problem. Though other numerical methods or solvers can be used, we apply Newton's method as it proves to be very efficient and accurate as applied to this equation.

Without loss of generality we will drop the subscript 1_i since the equation is of the same form for all i, but remembering that the corresponding equation must be solved at each i on surface A_1 with the corresponding information.

Let

$$\begin{aligned} T^* &= T(t+\Delta t), \\ T_o &= T(t), \\ g(T^*) &= 2C^2B^4\Delta t + \frac{1}{2C}\ln\left|\frac{T^*-C}{T^*+C}\right| \\ &- \frac{1}{C}\arctan\left(\frac{T^*}{C}\right) - \frac{1}{2C}\ln\left|\frac{T_o-C}{T_o+C}\right| + \frac{1}{C}\arctan\left(\frac{T_o}{C}\right), \end{aligned} \tag{19}$$

so that

$$g'(T^*) = \frac{2C^2}{T^{*4}-C^4}. \tag{20}$$

Newton's method is given by:

$$\begin{aligned} T_o^* &= T_o, \\ T_{n+1}^* &= T_n^* - \frac{g\left(T_n^*\right)}{g'\left(T_n^*\right)}. \end{aligned} \tag{21}$$

Applying Newton's method to the heat balance equation we arrive at a recursive algorithm for solving the temperature for the time advance Δt. For the numerical simulations discussed in this paper we used $m = n = 22$, for the number of divisions of the wafer surface (including the wafer, space and guard ring) and for the number of divisions of the showerhead surface (including the showerhead and any space left open). For this equation and typical RTP variable values, we need between 3 to 5 iterations of Newton's method to achieve a solution of the ODE, accurate to within computer round-off error.

4 Data and simulation

For the numerical experiments various input parameters are needed. Unless the variation of these parameters is expressed in the legend, then the input parameters that are used are those defined below.

The specific heat of silicon varies greatly for the temperature ranges considered in the RTP process run, so the values used have been extracted from data tables in the "Materials Handbook", [1]. The variation of density with temperature does not vary as significantly as a function of temperature as the heat capacity does; these values have also been extracted from the "Materials Handbook", [1].

"The viscosity of gases and most liquids increases slowly with pressure. Since the change in viscosity is only a few percent up to 100 atm," cf. [6], pressure effects will be neglected. Gas viscosity increases with temperature; a common approximation and what is used in the model of this paper is Sutherland's law:

$$\frac{\mu}{\mu_o} = \frac{\left(\frac{T}{T_o}\right)^{3/2}(T_o+S)}{T+S}, \tag{22}$$

where μ_o is a known viscosity at a known absolute temperature T_o. For nitrogen at a temperature of $T_o = 273.11K$, $\mu_o = 0.1663mP = 0.1663 \times 10^{-4}\ kg/m \cdot s$ and $S = 106.67K$. The constant S is fit to the available data, and is accurate for a wide range of values. "For temperatures between 180^oR and 2700^oR ($100\,\mathrm{K} - 1500\,\mathrm{K}$) the error associated with this approximation is $\pm 2\%$,", cf. [6].

Thermal conductivity is a thermodynamic property and varies with temperature and pressure, as does viscosity. The conductivity is a function of the Prandtl number which is nearly constant for gases and equal to 0.72. From the definition of the Prandtl number: $Pr = c_p\mu/k_{\mathsf{N}}$, solving for k_{N} leads to: $k_{\mathsf{N}} = c_p\mu/Pr$, where $c_p = \gamma R/(\gamma - 1)$ and R is the gas constant with value of 296.8 for nitrogen; γ is the ratio of the specific heats. The values at atmospheric pressure of the specific heats at high temperatures are extracted from the CRC "Handbook of Chemistry and Physics,", cf. [4]. Taking the ratio of the specific heats results in a value for γ of approximately 1.35 at these temperatures. The viscosity μ as described above may be inserted here to obtain the conductivity k.

The temperature gradient above and below the wafer are needed in order to solve the heat balance equation, and so a linear approximation to this is used here. Above the wafer, let the distance between the wafer and the showerhead be d_{aw}. At a time t^* the heat gradient at the i^{th} ring above the wafer is given by the temperature difference between the constant temperature of the showerhead, T_{sh}, and the temperature at the i^{th} ring, $T_i(t^*)$, divided by d_{aw},

$$\left.\frac{\partial T}{\partial y}\right|_{aw} = \frac{T_{sh} - T_i(t^*)}{d_{aw}}. \tag{23}$$

Below the wafer the distance between the wafer and the bottom of the chamber is $0.4572m$. At a time t^* the heat gradient at the i^{th} ring below the wafer is given by the temperature difference between the constant temperature of the chamber bottom: T_{cb} and the temperature at the i^{th} ring: $T_i(t^*)$, divided by d_{bw}

$$\left.\frac{\partial T}{\partial y}\right|_{bw} = \frac{T_i(t^*) - T_{cb}}{0.4572}. \tag{24}$$

4.1 Input parameters

The following are the input parameters unless otherwise noted in the discussion for any particular simulation.

- Power is increased linearly in time from zero to 28.9 W/cm^2 in 5 seconds, the power is then kept at this peak for 40 seconds and then the lamp is turned off.
- The reflectivity of the showerhead is 2%.
- The gap between the wafer and the guard ring is 0.25mm.
- The diameter of the silicon wafer is 200mm.
- The thickness of the silicon wafer is 0.7mm.

- The emissivity of the silicon wafer is 0.68.
- The guard ring width is 25mm.
- The showerhead radius is equal to 125.25mm, this equals the outer radius of the guard ring.
- The chamber height is 1cm.

The first data plot, Figure 3, displays the temperature profile at the center of the wafer using Vortek data and the numerical results for comparison. The two input parameters that are significantly different than those defined, are the chamber height and the power input. The chamber height used for these experiments is $5.715mm$. In the Vortek experiment the wafer is heated up in 2 seconds to peak power at $420Amps$. Then held for 19 seconds at $420Amps$. Then held at $410Amps$ for 11 seconds. This input translates to about 28.9 W/cm^2 corresponding to $420Amps$ and $410Amps$ is slightly lower at about 27.8 W/cm^2.

5 Discussion

We now compare the numerical results with the Vortek data for the set Vortek RTP geometry. Then we discuss the numerical results focusing on the effects of changing the chamber geometry in various ways.

Temperature profile: Figure 3 includes a graph of the temperature profile at the center of the wafer from the simulation of a process run. This profile is in accordance with typical temperature profiles as those found by Vortek from experimental data from a Sensarray wafer (thermocouple embedded) as shown in the same figure. There is a difference in the shape of the profile during the heating which may be improved by including a better model of the emissivity for temperatures lower than 700 °C. Further improvements may be possible if a better model for convection is used. **Temperature difference profile**: Figure 4 is the profile of the temperature difference between the center of the wafer to the edge through a simulation process run. From this graph we see that the largest differences in temperatures occur between the corner of ramp up and the peak steady state temperature reached by the wafer. Therefore in order to optimize the temperature uniformity along the wafer it will be useful to optimize the temperature uniformity focusing on the profiles at the peak temperatures. The saw-tooth profile that appears in the cooling stage in Figure 4 is not a physical possibility, it is a result of the numerical errors at each time step.

Temperature drop off from wafer center to edge: Figure 5 shows the profile on the wafer starting at the center of the wafer along to the edge. This shows the typical profile of how the temperature varies from the center to the edge of the wafer at the peak temperature, at time $t = 40s$. The temperature drop-off that we see here is because the center of the wafer simply "sees" more of the showerhead, and so is exposed to more of the radiant energy reflected from it. The center will be the hottest point and each point along the wafer will be exposed to less and less

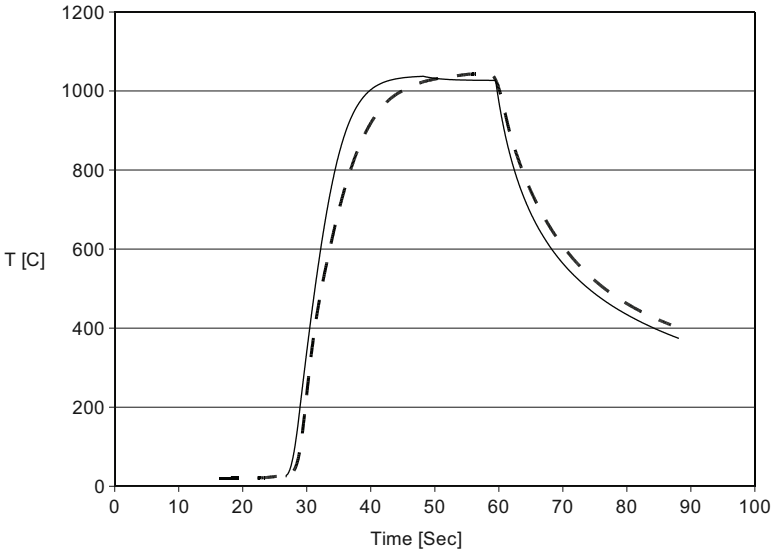

Figure 3: *Vortek data at wafer center (dashed line) and numerical data at wafer center (solid line).*

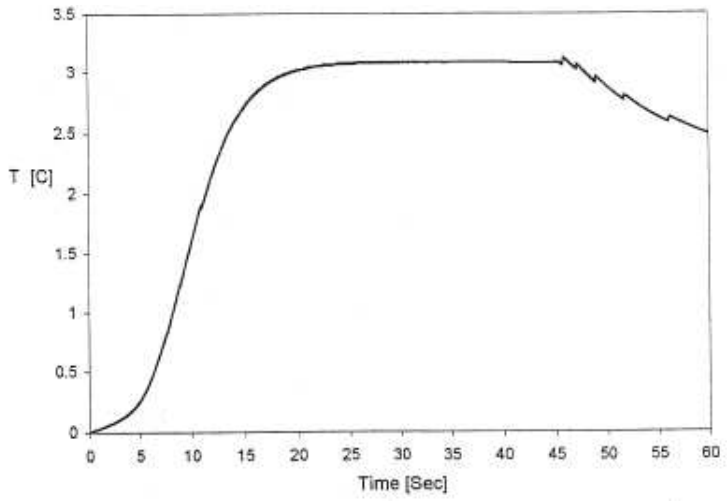

Figure 4: *Temperature difference from wafer center to edge*

radiation as you go out. The closer you are to the center, the smaller the drop-off. The reason a guard ring is used around the wafer is that it can take the drop-off effects, thus making the wafer more uniform. In figures 6-9 we graph the temperature drop-off at the peak temperature, as it will

be useful to show the effects of varying geometries and reflectivities.

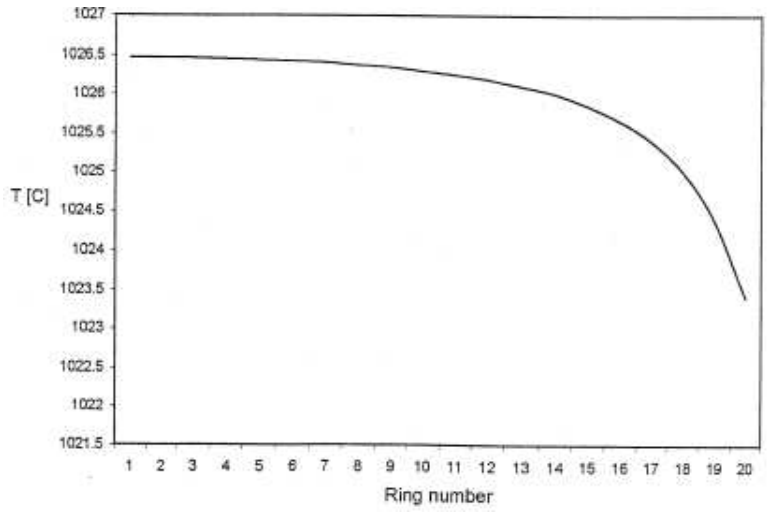

Figure 5: *Temperature drop off at time $t = 40s$*

Different showerhead diameters: The graph of Figure 6 shows the temperature profiles of varying showerhead diameters, at time $t = 40s$. When the showerhead diameter is smaller than the outer diameter of the guard ring, most of the energy is wasted and uniformity improvements are not so noticeable. However, uniformity improvements are more apparent with a larger showerhead diameter compared with a diameter that is the same size as the outer diameter of the guard ring. Thus, for better uniformity it is important to have the showerhead diameter the same size, or larger, than the outer diameter of the guard ring.

Different guard ring widths: Figure 7 shows the temperature profiles of varying guard ring widths at time $t = 40s$. From this graph we see that the best uniformity occurs along the wafer when the guard ring width is largest, given financial and mechanical constraints.

Different reflectivities: Figure 8 shows three different temperature profiles corresponding to different showerhead reflectivities, which would correspond to different showerhead materials, at time $t = 40s$. A perfect black showerhead would have a reflectivity of 0%, however in practice it is only possible to attain a 2% reflective material. It is clear from this graph that the 2% reflective showerhead leads to the most uniform temperature profile and would thus be the best. However, as mentioned previously, there are constraints that would lead a manufacturer to avoid such a low reflective material. For example, if you use the lower reflective material, you will need to use more energy from the lamp source in order to achieve the same peak temperature necessary for the process.

Different chamber heights: Figure 9 is a graph that shows the temperature profiles along the wafer for various chamber heights at time $t = 40s$. It is clear in the legend that the smaller

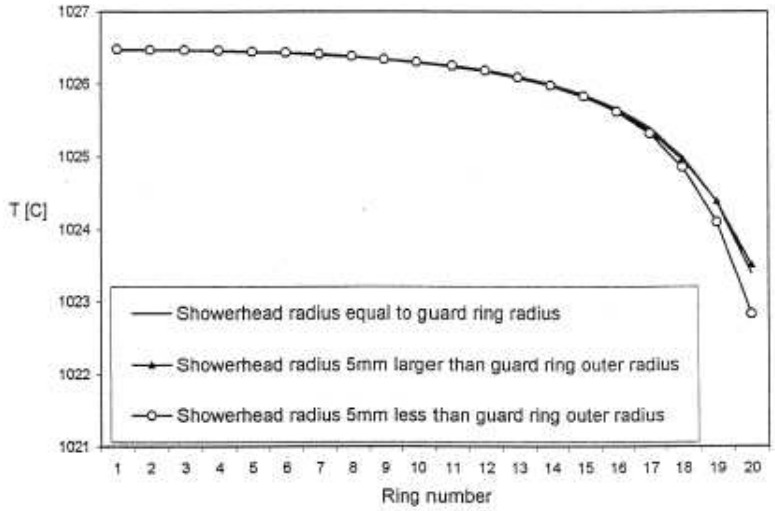

Figure 6: *Temperature drop off for different showerhead radii at time $t = 40s$*

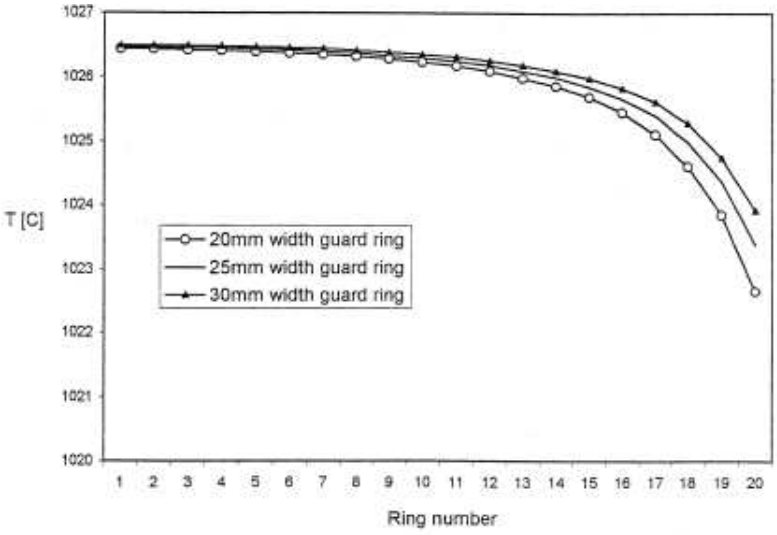

Figure 7: *Temperature drop off for different guard ring widths at time $t = 40s$*

chamber height minimizes the temperature difference from the center of the wafer to the edge of the wafer.

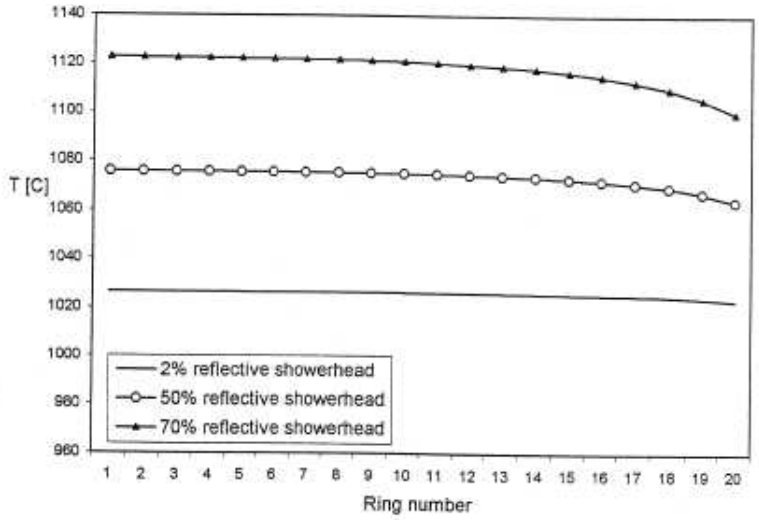

Figure 8: *Temperature drop off for different reflectivities at time $t = 40s$*

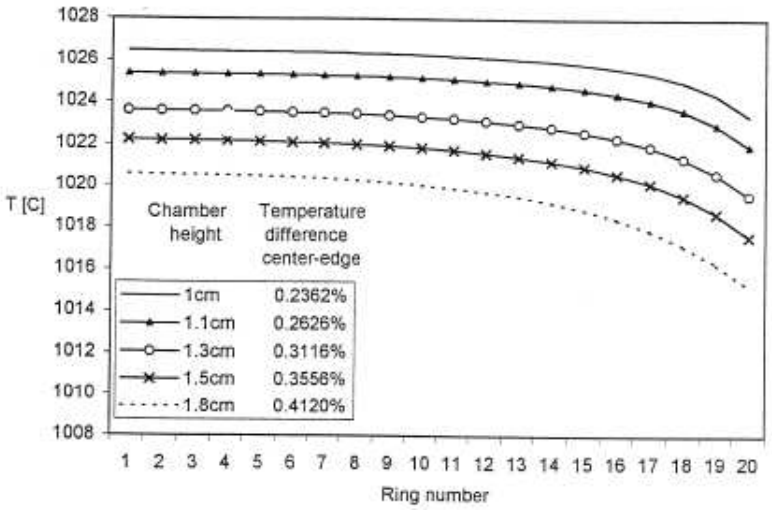

Figure 9: *Temperature drop off for different chamber heights at time $t = 40s$*

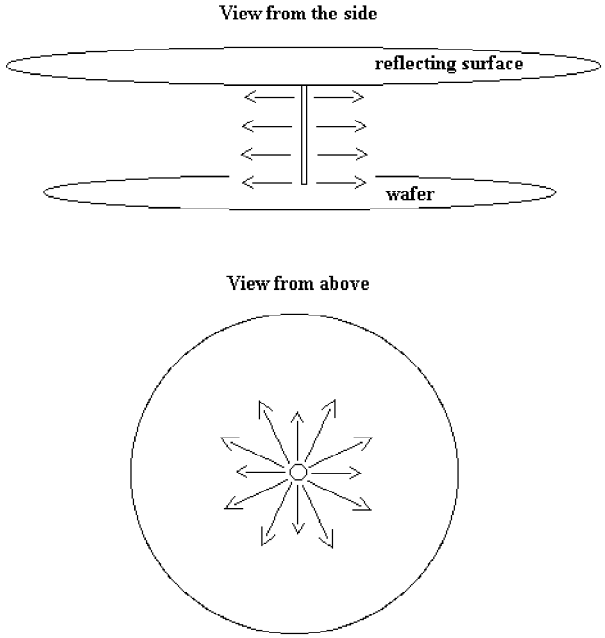

Figure 10: *Uniform axially symmetric flow profile*

6 Conclusion

This simulation data is in accordance with typical temperature profiles as those found by Vortek from experimental data from a Sensarray wafer. In order to improve temperature uniformity on the wafer, the showerhead should have the same radius or a larger radius than the guard ring outer radius. For practical purposes however the chamber should be maintained relatively small, less than $300mm$ in diameter so the radius of the showerhead should be kept below these limits. The larger the guard ring the more uniform the temperature will be, and so it is desirable to use as large a guard ring as possible. For practical purposes the guard ring should be no more than about $2.5cm$ in width, since beyond this point too much power is needed to keeping the guard ring hot making it an expensive process. The lower the reflectivity the more uniform the temperature on the wafer. However, the reflector minimizes the amount of power needed from the lamp to achieve the peak temperatures, and so some reflectivity is useful to reduce the amount of power needed and in practice any material employed will have some reflectivity. Ideally the smallest chamber height attains the best temperature uniformity. In practice there will be a flow included in the RTP process to further improve temperature uniformity. If the flow is impinging on the wafer surface, a chamber height that is too small will create cool spots, as those found by Vortek in experiments in which the chamber height was small. If however the flow is parallel to the wafer, this would resolve the cold spots and one can take advantage of the improved uniformity resultant of the

small chamber height. Gas flows are typically used in RTP machines to reduce the temperature non-uniformities created by the reflections in the chamber. Since it is desirable to take advantage of the uniformity resultant of a small distance between the showerhead and the wafer we recommend a uniform and axially symmetric profile coming from a thin pipe source connected to the reflecting showerhead, as shown in Figure 10. The flow would be tangential to the wafer and would still take advantage of the uniformity improvement of the reflector and circular wafer, but removes the possibility of cold spots when flow is fast enough to make the profile fully developed. Making the flow fully developed removes the possibility of convective cells. The flow will then cool the center of the wafer more than the edges (where it is needed) since the velocity will be higher at the center and will thus take more energy away from the hotter center, aiding in uniformity.

Acknowledgements

The first author would like to thank the Pacific Institute for the Mathematical Sciences which supported this research in the form of a research assistantship at the University of British Columbia. The first author would also like to thank Prof. Huaxiong Huang, Prof. Carl Ollivier-Gooch, Prof. Brian Seymour and Marcel Lefrancois for many valuable discussions and support as supervisors throughout her research on this topic.

References

[1] G.S. Brady, *Materials Handbook*, McGraw-Hill, New York, 1972. 9

[2] A.J. Chapman, *Heat transfer*, The Macmillan Company, London, 1967. 3, 4

[3] F. Kreith, *Radiation Heat Transfer for Spacecraft and Solar Power Plant Design*, International Textbook Company, Scranton, Pennsylvania, 1962. 4

[4] D.R. Lide, *CRC Handbook of Chemistry and Physics*, CRC press, New York, 1993. 10

[5] T. Sato, *Spectral Emissivity of Silicon*, Japanese Journal of Applied Physics **6** (1967), 339–347. 3

[6] F.M. White, *Fluid mechanics*, McGraw-Hill, New York, 1986. 9, 10

A Model parameters

Quantity	**Symbol**	**Si Units**
Emissive power	W	W/m^2
Radiosity	J	W/m^2
Irradiation	G	W/m^2
Total hemispherical emissivity	ϵ	
Temperature	T	K
Absorptivity	α	
Reflectivity	r	
Transmissivity	τ	
Area	A	m^2
Mass density	ρ	kg/m^3
Heat capacity (Specific heat)	C_p	$J/(kg \cdot K)$
Thermal conductivity	k	$W/(m \cdot K)$
Shape factor	F_{12}	
Time	t	s
Time step (Change in time)	Δt	s
Thickness of silicon wafer	h_{Si}	m
Constant	**Symbol**	**Value**
Stefan-Boltzmann constant	σ	$5.67E-8\ W/(m^2 \cdot K^4)$